ACS Infectious Diseases

pubs.acs.org/journal/aidcbc

Letter

# Characterization of Serine Hydrolases Across Clinical Isolates of Commensal Skin Bacteria *Staphylococcus epidermidis* Using Activity-Based Protein Profiling

Laura J. Keller, Christian S. Lentz, Y. Erin Chen, Rebecca J. Metivier, Eranthie Weerapana, Michael A. Fischbach, and Matthew Bogyo*

Cite This: *ACS Infect. Dis.* 2020, 6, 930−938

Read Online

ACCESS | Metrics & More | Article Recommendations | Supporting Information

**ABSTRACT:** The bacterial genus *Staphylococcus* comprises diverse species that colonize the skin as commensals but can also cause infection. Previous work identified a family of serine hydrolases termed fluorophoshonate-binding hydrolases (Fphs) in the pathogenic bacteria *Staphylococcus aureus*, one of which, FphB, functions as a virulence factor. Using a combination of bioinformatics and activity-based protein profiling (ABPP), we identify homologues of these enzymes in the related commensal bacteria *Staphylococcus epidermidis*. Two of the *S. aureus* Fph enzymes were not identified in *S. epidermidis*. Using ABPP, we identified several candidate hydrolases that were not previously identified in *S. aureus* that may be functionally related to the Fphs. Interestingly, the activity of the Fphs vary across clinical isolates of *S. epidermidis*. Biochemical characterization of the FphB homologue in *S. epidermidis* (SeFphB) suggests it is a functional homologue of FphB in *S. aureus*, but our preliminary studies suggest it may not have a role in colonization *in vivo*. This potential difference in biological function between the Fphs of closely related staphylococcal species may provide mechanisms for specific inhibition of *S. aureus* infection without perturbing commensal communities of related bacteria.

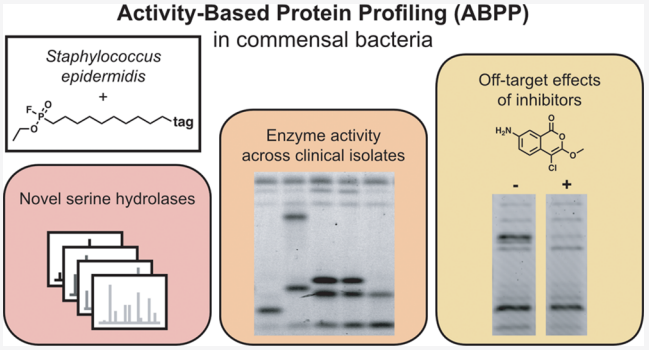


**KEYWORDS:** *Staphylococcus epidermidis, activity-based protein profiling, serine hydrolases, commensal bacteria*



Bacteria from the genus *Staphylococcus* are some of the most prevalent bacteria isolated from human skin,[1,2] especially abundant in the nasal passage and other moist areas.[3−5] They often exist as pathobionts in the skin microbiome that can be major human health threats if they evade host defenses. The most extensively studied staphylococcal species is *Staphylococcus aureus*, a native member of the nasal flora in 30% of the population that can cause endocarditis and sepsis upon bloodstream exposure.[6] Of growing interest is the related yet less virulent *Staphylococcus epidermidis*,[7] a commensal bacterium frequently isolated from the skin and also a leading cause of nosocomial infections.[8,9] Extensive efforts have tracked the epidemiology of healthy and infection-derived *S. epidermidis* clinical isolates with marker gene[10] and genomic-based[11,12] techniques and correlated the clustering of these strains with various functional assays relevant to their pathogenic potential.[13] To further understand the biology of these strains, it would be useful to apply a profiling technique that is directly related to the function of the bacteria.

One such technique is activity-based protein profiling (ABPP), a chemoproteomic technique that utilizes chemical probes that can covalently modify the active site of catalytically active enzymes and thus label in parallel all active enzymes of a particular class with a tag.[14] Initially developed as a profiling platform in mammalian systems,[15−17] ABPP has been applied to pathogenic bacteria to identify novel members of an enzyme class,[18] track changes in enzyme activity across *in vitro* conditions mimicking infection,[19] discriminate between closely related strains,[20] screen for selective inhibitors within a class of enzymes,[21] and characterize bacterial enzymes active in *in vivo* infection models.[22] Previously, we used a fluorophosphonate (FP)-based activity-based probe on *S. aureus* grown in biofilm-promoting conditions to identify a family of 12 serine hydrolases, named fluorophoshonate-binding hydrolases (Fphs), that are active under biofilm-promoting conditions.[23] One of these enzymes, FphB, is a lipid esterase that is important for *S. aureus* colonization of the liver and heart in a systemic infection mouse model.[23]

**Received:** March 2, 2020
**Published:** April 16, 2020




https://dx.doi.org/10.1021/acsinfecdis.0c00095
*ACS Infect. Dis.* 2020, 6, 930−938

FphB is a promising candidate target for the development of small molecule inhibitors, such as the chloroisocoumarin JCP251,[23] to treat systemic infections by *S. aureus*, but it is important to consider potential off-target effects on homologous enzymes in related bacteria. *S. epidermidis* as a commensal is known to prevent the colonization of[24] and even kill *S. aureus*[25] and tune the inflammatory and immune response during wound healing.[26−28] In order to not disrupt these beneficial functions of *S. epidermidis* as a commensal, it is important to understand how closely related serine hydrolases in *S. epidermidis* are to those in *S. aureus* and assess whether inhibitors developed for *S. aureus* infections will affect the viability of *S. epidermidis*. Here, we use a combination of bioinformatics and activity-based protein profiling in *S. epidermidis* to identify homologues of the Fphs, including FphB, in a laboratory strain as well as clinical isolates of *S. epidermidis*. Our findings demonstrate a high level of conservation of these hydrolases between the commensal and pathogenic strains of *Staphylococcus* but also identify additional serine hydrolases that are unique to *S. epidermidis*. We also find that activity levels of Fph enzymes are highly variable across clinical isolates and the function of FphB in *S. epidermidis* may be distinct from the function of its homologue in *S. aureus*.

Traditionally, microbiologists have used sequence-based bioinformatic approaches across related species to extrapolate information about uncharacterized enzymes. Using simple protein BLAST techniques with protein sequences from over 50 different species in the genus *Staphylococcus*, including *S. epidermidis*, we determined that, of the 12 serine hydrolases identified as FP-reactive enzymes in *Staphylococcus aureus*,[23] some such as FphH are well-conserved (Table S1). On the other hand, homologues, such as FphE, were identified in only about half of the species, not including *S. epidermidis* (Table S1).

We specifically focused on *Staphylococcus epidermidis*, a related and commonly studied skin commensal bacterial species. Of the 12 Fph enzymes in *S. aureus*, all but FphE and FphJ had at least one homologue in the reference strain *S. epidermidis* RP62A based on sequence homology. Interestingly, FphF and the two secreted lipases, Lipase 1 and Lipase 2, each had two homologues (Figure 1B, Table S1). Only two of these 13 bioinformatically predicted FP-reactive serine hydrolases have been previously characterized: SERP2388, a homologue of Lipase 2 also known as glycerol ester hydrolase D (GehD), which has lipolytic activity but can also bind to collagen,[29] and SERP2297, a homologue of Lipase 1 also known as gehSE1 that can hydrolyze short-chain triacylglycerols.[30]

To more comprehensively identify possible Fph homologues, we also performed mass spectrometry-based ABPP using a broadly reactive fluorophosphonate probe (Figure 1). We profiled 17 strains of *S. epidermidis*, including the reference strains RP62A and ATCC 12228 and clinical isolates from healthy volunteers and infected patients (Table S2). We labeled intact bacterial cells in late stationary phase with 5 $\mu$M FP-biotin (probe **1**, Figure 1A), and the samples were subsequently lysed, enriched for labeled proteins using a streptavidin resin, and analyzed by LC-MS/MS. Across the strains, 18 proteins were identified in at least four strains (Tables 1 and S3, Figure S1). However, in some strains, we detected fewer than half of these 18 proteins, even though at least 17 are encoded in the genome of each strain (except for NCTC 9865 and KPL1815, whose genomes have not yet been fully sequenced and assembled; Table S3). Consequently, it is important to note that failure to identify a protein in a given strain via ABPP and mass spectrometry is not sufficient to conclude that the enzyme is not expressed or active in that strain as the activity of some hydrolases may be regulated by other factors, including growth conditions and media composition, that prevent their labeling by the probe.

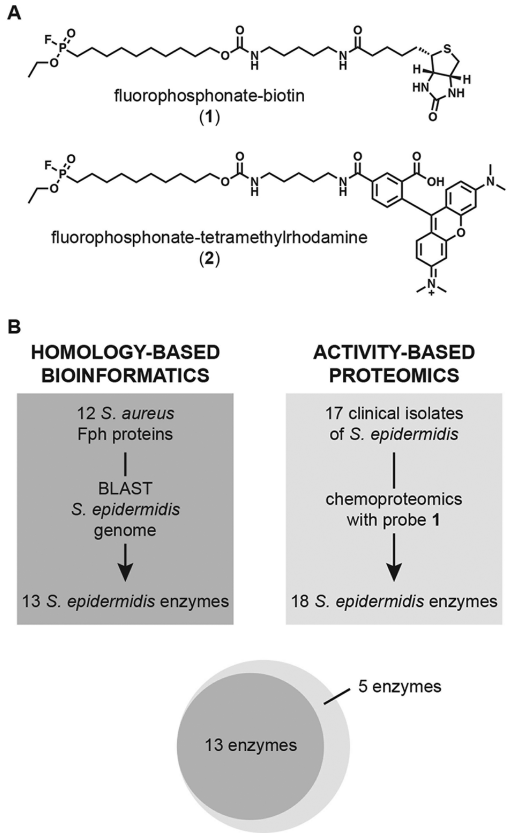


**Figure 1.** Comparison of bioinformatic and chemoproteomic approaches to identify fluorophosphonate-reactive serine hydrolases in *Staphylococcus epidermidis*. (A) Structures of fluorophosphonate (FP)-containing activity-based probes, FP-biotin (probe **1**) for mass spectrometry-based ABPP and FP-tetramethylrhodamine (probe **2**) for gel-based ABPP. (B) Workflow for homology-based bioinformatics and activity-based proteomics pipelines. The bioinformatic approach yielded 13 predicted FP-reactive serine hydrolases; ABPP identified the 13 predicted Fph enzymes and 5 additional serine hydrolases.

All 18 proteins are annotated as having putative $\alpha,\beta$-hydrolase or peptidase domains (Figure S1) and are predicted to be serine hydrolases by the ESTHER (http://bioweb.supagro.inra.fr/ESTHER/general?what=index) and/or MEROPS (https://www.ebi.ac.uk/merops/) databases (Table S3), suggesting that they are likely functional serine hydrolases. Of these 18 enzymes, all 13 bioinformatically predicted enzymes were detected by ABPP, but the functional profiling identified five additional active serine hydrolases in *S. epidermidis* that were not predicted by homology mapping from *S. aureus* alone (Table 1). Two of these additional five enzymes are previously characterized peptidases, ClpP[31] and glutamyl endopeptidase (GluSE).[32] Interestingly, the remaining three serine hydrolases are two putative esterases that were not identified as being active in biofilm-promoting conditions in *S. aureus* and a putative peptidase that does not have a homologue in *S. aureus*, demonstrating the importance of orthogonal, functional studies to complement bioinformatic approaches.

Because not all of the Fph enzymes in *S. epidermidis* were identified in every strain, we used gel-based ABPP with the fluorescent version of the FP probe used for the proteomic


https://dx.doi.org/10.1021/acsinfecdis.0c00095
ACS Infect. Dis. 2020, 6, 930−938

**Table 1. Fluorophosphonate-Reactive Serine Hydrolases Identified by Mass Spectrometry-Based ABPP[a]**

| *S. epidermidis* RP62A locus ID (protein name) | predicted molecular weight (kDa) | number of *S. epidermidis* strains in which it was identified | *S. aureus* NCTC 8325 homologue locus ID (protein name) | identified via homology-based bioinformatics |
|---|---|---|---|---|
| SERP2297 (GehSE1) | 77.4 | 17 | SAOUHSC_03006 (Lipase 1) | × |
| SERP2336 | 81.8 | 4 | SAOUHSC_03006 (Lipase 1) | × |
| SERP2388 (GehD) | 72.2 | 13 | SAOUHSC_00300 (Lipase 2) | × |
| SERP0018 | 76.0 | 9 | SAOUHSC_00300 (Lipase 2) | × |
| SERP2035 | 52.9 | 4 | SAOUHSC_02751 (FphA) | × |
| SERP2109 (SeFphB) | 37.4 | 12 | SAOUHSC_02844 (FphB) | × |
| SERP0869 | 36.4 | 14 | SAOUHSC_01279 (FphC) | × |
| SERP1788 | 32.8 | 7 | SAOUHSC_02448 (FphD) | × |
| SERP2245 | 29.0 | 17 | SAOUHSC_02962 (FphF) | × |
| SERP2354 | 29.2 | 7 | SAOUHSC_02962 (FphF) | × |
| SERP1354 | 30.5 | 6 | SAOUHSC_01912 (FphG) | × |
| SERP0449 | 28.3 | 17 | SAOUHSC_00802 (FphH) | × |
| SERP0090 | 28.2 | 17 | SAOUHSC_00417 (FphI) | × |
| SERP0603 | 29.2 | 15 | SAOUHSC_00950 | |
| SERP0309 | 40.0 | 14 | SAOUHSC_00661 | |
| SERP0436 (ClpP) | 21.4 | 9 | SAOUHSC_00790 (ClpP) | |
| SERP1397 (GluSE) | 30.8 | 6 | SAOUHSC_00988 (SspA) | |
| SERP2401 | 27.8 | 4 | | |

[a]Homologues of the *S. aureus* Fph enzymes FphE and FphJ were not identified via bioinformatic analysis of the genome or mass spectrometry-based ABPP in *S. epidermidis*.

experiments, FP-tetramethylrhodamine (probe **2**, Figure 1A), to directly visualize the labeling of the serine hydrolase activities across the strains (Figures 2A and S2). These data confirm that overall levels of labeled hydrolases vary across the different clinical isolates and several labeled species appear only in some of the strains. The reason for this divergence in activities among strains may be the result of their isolation from different locations on the body with different microenvironments. We cannot make any specific conclusions about this due to the small sample numbers for each location, but studies on larger cohorts of clinical isolates may help to address this finding. While it is difficult to predict the clinical relevance of the distinct enzyme activity levels, the clustering of these isolates based on their genomic content,[28,33] which is often used in epidemiology studies to classify strains into phylogenetic groups,[11] does not correlate with the clustering based on the patterns of serine hydrolase activity (Figure 2B). This suggests that genomic-based stratifications overlook at least some aspects of functional diversity in these strains that is made apparent by enriching for the activity of this class of enzymes. This natural variation in serine hydrolase activity may help to uncover the importance of hydrolysis of various proteinaceous and fatty acid substrates for survival on different skin surfaces and even in the blood.

Because of the role of FphB in infection in *S. aureus*, we were interested in understanding whether its homologue in *S. epidermidis* has a similar function (for clarity, FphB in *S. aureus* will be referred to as SaFphB and the FphB homologue in *S. epidermidis* will be referred to as SeFphB). By sequence, SeFphB contains the canonical serine hydrolase Ser-Asp-His catalytic triad and the Gly-Xaa-Ser-Yaa-Gly lipase domain[34,35] (Figure 3A). To determine if SeFphB is a functional homologue of SaFphB, we used the strain NIH LM087, as it is well studied in the context of *S. epidermidis* commensalism for its ability to induce the recruitment of $CD8^+$ T cells.[36,37] We generated a "scarless" deletion of SeFphB in the NIH LM087 strain (Δ*fphB*). Labeling with probe **2** confirmed the loss of a 37 kDa protein, corresponding to the predicted size of SeFphB (Figure 3B). In further support of the identity of this protein as SeFphB, pretreatment of intact wild-type cells with 1 μM JCP251 (inhibitor **3**, Figure 3B), a selective inhibitor designed against SaFphB,[23] blocked labeling of the 37 kDa SeFphB band but also blocked labeling of two additional proteins, suggesting that it has other off-target effects in *S. epidermidis* (Figure 3B). We can extrapolate to identify the band corresponding to SeFphB in the remaining strains (denoted by an asterisk in Figure 2A), and interestingly, the activity of this enzyme varies across the *S. epidermidis* strains.

To further characterize the function of SeFphB, we recombinantly expressed the enzyme in *Escherichia coli* and measured its activity against a panel of fluorogenic substrates (Figure S3) previously used to characterize the substrate selectivity of SaFphB.[23] Similar to SaFphB, SeFphB can cleave fatty acid esters but not phosphate, phosphonate, or glycosidic substrates (Figure 4A). It also prefers $C_4$, $C_7$, and $C_8$ chain-length substrates, but unlike SaFphB,[23] it is capable of processing acetate ester (Figure 4A). As a control, the catalytic-dead mutant, S176A, does not cleave any of the substrates (Figure 4A). Similar to SaFphB,[23] disruption of the expression or inhibition of SeFphB by inhibitor **3** does not affect exponential growth rate *in vitro* (Figure 4B).

We previously demonstrated that the loss of SaFphB led to reduced infection of specific organs in a mouse model of systemic *S. aureus* infection.[23] We therefore wanted to determine if SeFphB might also play a role during *in vivo* colonization of the skin, the anatomical niche most commonly occupied by this bacterium. We utilized a mouse model commonly used to measure the recruitment of immune cells in response to the introduction of *S. epidermidis* to the skin,[27,28] as it is a non-native member of the mouse skin microbiome.[38] In this model, colony-forming units (CFUs) of *S. epidermidis* are measured to quantify the association and maintenance of *S. epidermidis* on mouse skin. In comparison to the naive controls, bacteria in all three conditions successfully associated with the mouse skin, but there was no significant difference between wild-type, Δ*fphB*, and inhibitor **3** pretreatment (Figure 4C). However, the high levels of variability in each condition


https://dx.doi.org/10.1021/acsinfecdis.0c00095
ACS Infect. Dis. 2020, 6, 930−938

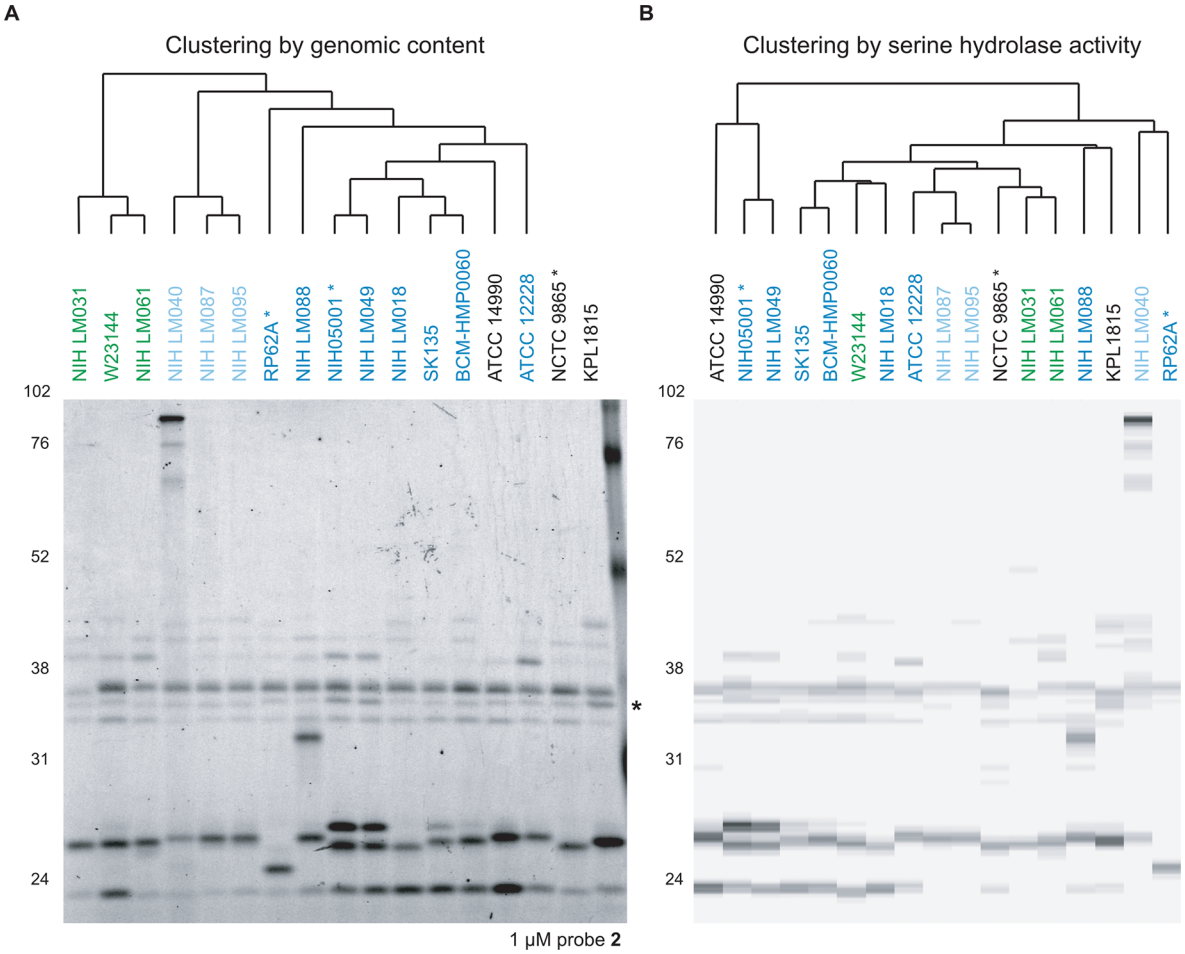


**Figure 2.** Diverse activities of serine hydrolases across *S. epidermidis* strains. (A) Representative in-gel fluorescence of labeling of intact bacterial cultures of clinical isolates of *S. epidermidis* with probe **2**. Strains were organized by phylogenetic analysis of their genomic content.[28,33] Strains NCTC 9685 and KPL1815 are not clustered because their genomes have not been sequenced. The asterisk denotes the location of the band corresponding to SeFphB; the remaining bands are not annotated because their identities are unknown. (B) Clustering of clinical isolates by quantification of in-gel fluorescence banding patterns. Strains are colored by their phylogenetic group (green, group B; light blue, group C; dark blue, group A; black, unknown),[11] and asterisks denote strains derived from infected patients (Table S2).

demonstrate the nonquantitative nature of this model and highlight the need for more robust *in vivo* models to assess commensalism on the skin.

Using activity-based protein profiling, we were able to identify 18 fluorophosphonate-reactive serine hydrolases in the commensal bacteria *Staphylococcus epidermidis*, 13 of which are homologues of Fph enzymes identified in the related pathogenic bacteria *S. aureus*. While the activity of these enzymes varied across clinical isolates derived from healthy volunteers and infected patients, the profiles of serine hydrolase activity do not directly map to genome-based clustering. Marker gene- and genome-based tools are powerful in the context of epidemiology, but profiling approaches that assess the actual function of bacterial strains may further help elucidate their biological differences. Furthermore, we demonstrated that, while SeFphB is a functional homologue of the *S. aureus* virulence factor SaFphB *in vitro*, it may not have an effect on the colonization capability of *S. epidermidis*. However, more robust *in vivo* models for understanding bacterial commensalism in the skin need to be developed to conclusively determine whether small molecules designed to target SaFphB to treat *S. aureus* infections can be developed without disrupting related commensal strains such as *S. epidermidis*.

Overall, this work demonstrates the power of using activity-based protein profiling combined with informatics-based analysis for the study of commensal bacteria. While ABPP only captures a subset of enzyme activity, broadly reactive activity-based probes, from the fluorophosphonate probes used in this study to nucleotide acyl phosphate probes that label ATP-binding enzymes,[39] are able to profile changes in activity across large classes of enzymes in many diverse bacterial strains and cultivation conditions. In doing so, it provides a rapid way to confirm protein annotations in often poorly characterized bacterial genomes. While we have focused on serine hydrolase targets here, this general approach could be applied to perform a similar analysis for virtually any enzyme class for which general activity-based probes are available. Additionally, ABPP allows direct screening of the cross-reactivity of inhibitors within related enzyme families, in a species of interest as well as in highly related species. As we move toward a goal of using drugs to target pathogenic bacteria, it is important to consider the potential impact on closely related commensal bacteria that have beneficial functions for human health. The application of ABPP to commensal bacteria will enable a more detailed understanding of potential off-species targets.


https://dx.doi.org/10.1021/acsinfecdis.0c00095
ACS Infect. Dis. 2020, 6, 930−938


**Figure 3.** SeFphB, the *S. epidermidis* homologue of FphB in *S. aureus* (SaFphB), can be knocked out and is inhibited by a SaFphB-selective inhibitor. (A) Sequence alignment of SaFphB and SeFphB. Asterisks denote a shared residue while colons and periods refer to similar residues at a given position. In gray, the lipase domains of both SaFphB and SeFphB are highlighted. The predicted residues of the catalytic triad, Ser176/Asp223/His300, are highlighted in red. (B) Image of in-gel fluorescence labeling of NIH LM087 wild-type and Δ*fphB* strains with 1 μM probe **2**. The third lane shows competitive pretreatment of wild-type cells with 1 μM inhibitor **3**. The asterisk indicates the location of the band corresponding to SeFphB that disappears in the Δ*fphB* strain, and the arrowheads indicate the positions of two additional proteins that are competed by inhibitor **3**.

## METHODS

**Mice.** Wild-type female C57BL/6 specific pathogen-free mice were purchased from Taconic Farms. All mice were maintained at an American Association for the Accreditation of Laboratory Animal Care (AAALAC)-accredited animal facility at Stanford University. Experiments were performed under the animal study protocol #32872 approved by the Stanford Laboratory Animal Care Committee.

**Bacterial Strains and Growth Conditions.** All bacterial strains used in this study are summarized in Table S2. Strains were cultured in either Difco tryptic soy broth (TSB; Sigma) or brain-heart infusion broth (BHI; Remel). All strains were struck from frozen glycerol stocks to be incubated on agar-containing plates at 37 °C, and then, colonies were picked to inoculate liquid cultures, which were incubated by shaking at 37 °C and 200 rpm.

For growth curves, overnight cultures were diluted to an $OD_{600}$ of 0.02 in BHI, and $OD_{600}$ measurements were made every 10 min for 12 h on a Cytation 3 imaging reader (BioTek). Exponential growth rate was calculated as the slope of the linear portion of the natural log-transformed data.

**Bioinformatic Analysis of Fphs.** To understand the conservation of the *Staphylococcus aureus* Fph enzymes, for each of the 52 species in the genus *Staphylococcus* whose genome has been assembled and published on NCBI, the genome of a representative strain was retrieved (January 10, 2020). All 12 FP-reactive enzymes identified in *S. aureus* NCTC 8325[23] were queried against each strain by Protein−protein BLAST (2.9.0+), requiring an e-value of less than $1 \times 10^{-40}$.

To identify the *S. aureus* homologues of the FP-reactive enzymes in the *S. epidermidis* clinical isolates, the sequence of each protein in *S. epidermidis* RP62A was used as a blastp (protein−protein blast, https://blast.ncbi.nlm.nih.gov) query sequence against *S. aureus* NCTC 8325. In order to be considered a homologue, the alignment had to have an e-value of less than $1 \times 10^{-40}$, and the *S. epidermidis* and *S. aureus* homologues had to be reciprocal best hits.

To identify the catalytic triad in SeFphB, the sequences of FphB in *S. aureus* NCTC 8325 and *S. epidermidis* NIH LM087 were aligned using Clustal Omega (https://www.ebi.ac.uk/Tools/msa/clustalo/). The predicted active-site serine within the lipase domain was confirmed by recombinant enzyme activity. The predicted active-site aspartate and histidine residues were corroborated by structural homology mapping with Phyre2 to a putative esterase from *Staphylococcus aureus* (PDB: 3D7R) (Figure S4).

**Mass Spectrometry-Based Activity-Based Protein Profiling Sample Preparation and Analysis.** Each strain of *S. epidermidis* was grown overnight to stationary phase in 3 mL of TSB and then concentrated to 1 mL. The samples were incubated with 5 μL of 1 mM probe **1** (5 μM final concentration) for 30 min at 37 °C and 300 rpm. To help solubilize the protein, 100 μL of 1% SDS in PBS and 100 μL of 10% TritonX-100 were added to each sample, and then, the samples were transferred to 2.0 mL O-ring tubes filled halfway with 0.1 mm glass beads. Samples were lysed by bead-beating in a prechilled aluminum block (3 × 50 s, with 2 min on ice in between), and the beads and cell debris were pelleted by centrifugation. The lysates were transferred to 1.5 mL Eppendorf tubes; 100 μL of 10% TritonX-100 in water was added, and the samples were incubated on a rotator for 1 h at 4 °C. The total volume of each lysate was brought to 2 mL with PBS and loaded onto a pre-equilibrated Sephadex G-25 PD-10 column (GE Healthcare). The protein was eluted with 3.5 mL of PBS; 184 μL of 10% SDS in water (0.5% final concentration) was added, and the samples were boiled for 8 min at 90 °C. While the samples cooled, aliquots of 100 μL of a 50% (v/v) streptavidin−agarose slurry were washed 3 times in 1 mL of PBS,


https://dx.doi.org/10.1021/acsinfecdis.0c00095
ACS Infect. Dis. 2020, 6, 930−938

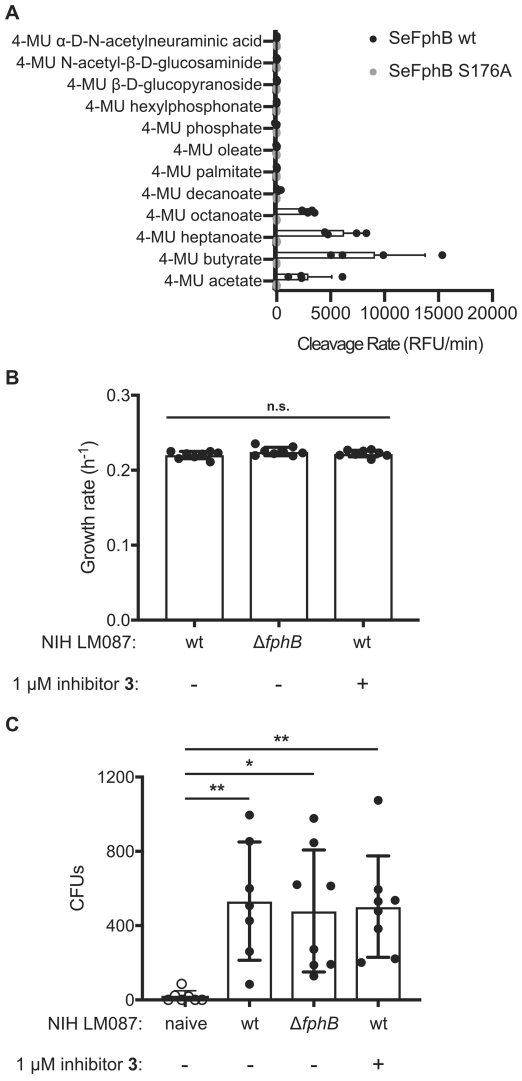


**Figure 4.** *In vitro* and *in vivo* characterization of SeFphB. (A) Processing of 4-methylumbelliferone (4-MU)-conjugated substrates by recombinant wild-type and catalytic-dead (S176A) SeFphB as measured by cleavage rate (relative fluorescent unit (RFU)/min). Each point represents an individual experiment, and bars show mean ± standard deviation ($n \geq 3$). (B) Exponential growth rate of NIH LM087 wild-type, with or without 1 $\mu$M inhibitor **3** pretreatment, and Δ*fphB* strains. Shown here is a representative experiment, with each point representing a technical replicate and bars showing mean ± standard deviation. (C) Colony-forming units (CFUs) recovered from the ear and back of the head of mice 2 weeks after association with media (naive), NIH LM087 wild-type, with or without 1 $\mu$M inhibitor **3** pretreatment, and Δ*fphB* strains. Graph depicts pooled data (mean ± standard deviation; naive and wild-type, $n = 7$; Δ*fphB* and inhibitor **3**, $n = 8$) over two independent experiments.

with a final volume of 100 $\mu$L. The beads were transferred to the 15 mL conical tube containing the protein with 5 mL of PBS, and the samples were incubated on a rotator for 1 h at 25 °C. The samples were spun on a tabletop centrifuge and washed twice in 10 mL of 1% SDS, fresh 6 M urea, and PBS (each wash consisted of 8 min of rotation at 25 °C, a slow spin, and then aspiration). The slurry was transferred to a screw-capped Eppendorf tube, and the conical tube was rinsed with an additional 500 $\mu$L of PBS, which was added to the screw-capped Eppendorf tube. The beads were pelleted and resuspended in 500 $\mu$L of fresh 6 M urea. The samples were reduced (addition of 25 $\mu$L of 30 mg/mL dithiothreitol in PBS and heated for 15 min at 65 °C) and then alkylated (addition of 25 $\mu$L of 14 mg/mL iodoacetamide in PBS and incubated in the dark for 30 min at 37 °C). After adding 950 $\mu$L of PBS to each sample, the samples were centrifuged and washed in 1 mL of 100 mM triethylammonium bicarbonate (TEAB) buffer. The beads were resuspended in 204 $\mu$L of 100 mM TEAB buffer containing 2 $\mu$g of proteomics-grade trypsin (Sigma-Aldrich) and incubated overnight at 37 °C. The supernatant was transferred to a new 1.5 mL Eppendorf tube, and the beads were washed in 100 $\mu$L of 100 mM TEAB buffer, which was added to the same Eppendorf tube. The trypsin digests were analyzed by LC/LC-MS/MS as previously described.[40] The mass spectrometry proteomics data have been deposited to the ProteomeXchange Consortium via the PRIDE partner repository with the data set identifier PXD017758.

**Construction of the *S. epidermidis* NIH LM087 Δ*fphB* Strain.** The *S. epidermidis* NIH LM087 Δ*fphB* mutant strain was generated using a previously described method.[28] Briefly, the regions approximately 1 kb up- and downstream of the *fphB* gene (HMPREF9993_05403) were amplified using the following primers: LM087_fphB_1kbup_fwd, LM087_fphB_1kbup_rev, LM087_fphB_1kbdn_fwd, and LM087_fphB_1kbdn_rev (Table S4). The amplified flanking regions were assembled into the plasmid pIMAY (Addgene) using Gibson Assembly (New England Biolabs) and then transformed into the *S. epidermidis* NIH LM087 wild-type strain. Allelic recombinations that deleted the *fphB* gene without a genomic scar were selected for using a temperature shift to 37 °C and anhydrotetracycline. Successful deletions were confirmed via colony PCR using primers LM087_fphB_colony_up and LM087_fphB_colony_dn and sequencing with primer LM087_fphB_147bup (Table S4).

**Gel-Based Activity-Based Protein Profiling.** Two colonies of each strain, including NIH LM087 wild-type and Δ*fphB*, picked from growth on a BHI agar plate were inoculated in 2.5 mL of BHI broth overnight, and the optical density was adjusted to an $OD_{600}$ of 1.0 in a 96-well plate. For the profiling of serine hydrolase activity across strains of *S. epidermidis*, 100 $\mu$L of each sample was incubated with 1 $\mu$L of 100 $\mu$M probe **2** (1 $\mu$M final concentration) for 30 min at 37 °C, and 50 $\mu$L of PBS was added for lysis. To identify the target of inhibitor **3** in *S. epidermidis* NIH LM087, 150 $\mu$L of each sample is treated with 1.5 $\mu$L of DMSO or 100 $\mu$M inhibitor **3** (1 $\mu$M final concentration) for 1 h at 37 °C. Each sample was then incubated with 1.5 $\mu$L of 100 $\mu$M probe **2** (1 $\mu$M final concentration) for 30 min at 37 °C.

Labeled intact bacteria were lysed by bead-beating with 0.1 mm glass beads (BioSpec Products) in a prechilled aluminum block or in a 96-well plate (3 × 45 s, with 2 min on ice in between), and the beads and cell debris were pelleted by centrifugation. Lysate supernatants were boiled with SDS loading buffer and separated by SDS-PAGE. Tetramethylrhodamine fluorescence was imaged using the Cy3 channel on a Typhoon 9410 Imager (Amersham Biosciences).

To cluster the pattern of serine hydrolase activity of each clinical isolate, a vertical line was drawn in each lane of the in-fluorescence gel scan, and the intensity profile along the line was quantified using ImageJ. An intensity profile from a background portion of the gel was also generated. Each profile was segmented into approximately 120 bins, and the total intensity in each bin was used for cluster analysis. The background was subtracted from each profile, and any value below a threshold


https://dx.doi.org/10.1021/acsinfecdis.0c00095
ACS Infect. Dis. 2020, 6, 930−938

bin intensity of 8000 was considered to be background and set at 0. These thresholded profiles were then clustered using the pheatmap function in R.

**Cloning, Expression, and Purification of Recombinant SeFphB Wild-Type and S176A.** All enzymes were purchased from New England BioLabs. Genomic DNA was isolated from *S. epidermidis* NIH LM087 by boiling a colony in 10 μL of water for 5 min at 98 °C. This genomic DNA was used as a template for the PCR amplification of *fphB* (HMPREF9993_05403) with the Phusion polymerase and primers LM087_fphB_fwd_*Bam*HI and LM087_fphB_rev_XhoI (Table S4). *Bam*HI and XhoI restriction sites were added to the gene for cloning into the pET-28b(+) vector. To generate the catalytic dead S176A mutant, site-directed mutagenesis of the pET-28b(+)-SeFphB plasmid was performed with primers LM087_fphB_S176A_fwd and LM087_fphB_S176A_rev (Table S4). The plasmid was amplified with Pfusion polymerase, followed by DpnI digestion, PNK phosphorylation, and blunt-end ligation with T4 ligase. Successful cloning was confirmed by selection on 50 μg/mL kanamycin followed by Sanger sequencing.

The plasmids pET-28b(+)-SeFphB and pET-28b(+)-SeFphB_S176A (Table S5) were transformed into chemically competent *Escherichia coli* BL21 cells and selected for with 50 μg/mL kanamycin. Single colonies were picked and inoculated in a starter culture of 4 mL of 2xYT broth (Teknova) with 50 μg/mL kanamycin and then incubated with shaking overnight at 37 °C. The starter culture was added to 1 L of 2xYT broth with 50 μg/mL kanamycin, and at an $OD_{600}$ of 0.5, the cultures were transferred to be shaken at 20 °C; the expression of the plasmid was induced with isopropyl β-D-1-thiogalactopyranoside (IPTG; 0.5 mM final concentration) for 16 h. The cultures were centrifuged at 4000*g* for 30 min, and pellets were stored at −20 °C.

The purification of SeFphB wild-type and SeFphB S176A was performed as previously described.[23] Briefly, pellets were lysed in 35 mL of lysis buffer (50 mM $NaH_2PO_4$, 300 mM NaCl, 10 mM imidazole, pH 8.0) via sonication (6 × 10 s, 1.5 s pulse, 30% amplitude). Lysates were centrifuged at 16 000 rpm for 30 min at 4 °C, and the supernatant was incubated with 500 μL of Ni-NTA Agarose resin (QIAGEN) with shaking for 1 h at 4 °C. The resin was washed 3 times with 10 mL of wash buffer (50 mM $NaH_2PO_4$, 300 mM NaCl, 20 mM imidazole, pH 8.0) by centrifuging at 1000*g* for 2 min at 4 °C before being transferred to 2 mL Eppendorf tubes. The $His_6$- and T7-tagged proteins were eluted 3 times with 1 mL of elution buffer (50 mM $NaH_2PO_4$, 300 mM NaCl, 200 mM imidazole, pH 8.0) by centrifuging at 1000*g* for 2 min at 4 °C. The purity of each eluant was checked via SDS-PAGE and Coomassie stain and then pooled for further purification with the Novagen T7 Tag Affinity Purification Kit (EMD Millipore) as per the manufacturer's instructions. The activity of each eluant was checked via labeling with probe **2** (1 μM final concentration) for 30 min at 37 °C followed by boiling in SDS loading buffer, SDS-PAGE, and in-gel fluorescence. The eluants were combined, and 10K Amicon Ultra-15 10K Centrifugal Filters (EMD Millipore) were used to concentrate the samples while exchanging the buffer to 50 mM Tris-HCl, 300 mM NaCl, and 10% glycerol for long-term storage at −20 °C.

**Fluorogenic Substrate Enzyme Activity Assay.** Fluorogenic substrate assays were performed as previously described.[23] In a 384-well plate, 10 μM 4-methylumbelliferone (4-MU)-conjugated substrates (Sigma-Aldrich; Carbosynth) were combined with recombinant SeFphB wild-type or S176A (final concentration: 75 nM of total protein, 51 nM active wild-type enzyme as determined by active-site titration with inhibitor **3**) in 20 μL of 0.05% TritonX-100 in PBS. Fluorescence (ex/em: 365/455 nm) was measured every minute for 1 h in a Cytation 3 imaging reader (BioTek). Cleavage rate was calculated by subtracting background fluorescence from a no-enzyme control, and the average slope of the linear phase of the reaction was calculated as relative fluorescence units (RFU) per minute.

**Murine *In Vivo* Skin Association Model.** Overnight cultures of *S. epidermidis* NIH LM087 wild-type and Δ*fphB* in BHI were diluted to an $OD_{600}$ of 0.8. For inhibitor **3** treatment, diluted bacteria were incubated with 1 μM inhibitor **3** for 1 h with shaking at 37 °C. For each mouse, 5 mL of NIH LM087 wild-type, Δ*fphB*, wild-type + inhibitor **3**, or BHI broth as a control (naive) were topically associated with a sterile cotton swab on the ears and back of the head and neck of each mouse 2 days in a row. Thirteen days after the first association, mice were sacrificed, and sterile cotton swabs previously soaked in BHI broth were scrubbed on the ears and back of head and neck before being streaked onto Columbia Agar with 5% Sheep's Blood plates (Remel). The plates were incubated overnight at 37 °C, and the following day, colony-forming units (CFUs) were counted. One mouse associated with wild-type *S. epidermidis* was excluded from the analysis because a lawn of bacteria grew on the plate, preventing counting; thus, it was a clear outlier.

**Software.** Statistical analyses were performed using GraphPad Prism 8. Any effects of Δ*fphB* and inhibitor **3** treatment were calculated using a one-way ANOVA test followed by posthoc Tukey's multiple comparisons test, if appropriate. In-gel fluorescence images were analyzed in ImageJ 2.0.0. Clustering was performed using R. DNA sequence analysis was performed using SnapGene 5.0.7.

## ■ ASSOCIATED CONTENT

### Supporting Information

The Supporting Information is available free of charge at https://pubs.acs.org/doi/10.1021/acsinfecdis.0c00095.

Domain structure prediction of identified serine hydrolases; Coomassie stain of *S. epidermidis* clinical isolates; fluorogenic substrate library for screening substrate selectivity of SeFphB; predicted structure of the SeFphB active site; primers in this study; (PDF)

Conservation of Fph enzymes across the genus Staphylococcus (XLSX)

Strain information for strains of *S. epidermidis* in this study (XLSX)

Proteomics data from fluorophosphonate-based ABPP (XLSX)

### Special Issue Paper

This paper was intended for the Chemical Microbiology special issue [*ACS Infect. Dis.* 2020, *6* (4)].

## ■ AUTHOR INFORMATION

### Corresponding Author

**Matthew Bogyo** − *Pathology and Microbiology and Immunology, Stanford University School of Medicine, Stanford, California 94305, United States;* orcid.org/0000-0003-3753-4412; Email: mbogyo@stanford.edu



https://dx.doi.org/10.1021/acsinfecdis.0c00095
*ACS Infect. Dis.* 2020, 6, 930−938

### Authors

**Laura J. Keller** − *Departments of Chemical & Systems Biology, Stanford University School of Medicine, Stanford, California 94305, United States*

**Christian S. Lentz** − *Pathology, Stanford University School of Medicine, Stanford, California 94305, United States*

**Y. Erin Chen** − *Department of Bioengineering and ChEM-H, Stanford University, Stanford, California 94305, United States; Dermatology Service, Veterans Affairs Medical Center, San Francisco, California 94121, United States*

**Rebecca J. Metivier** − *Department of Chemistry, Boston College, Chestnut Hill, Massachusetts 02467, United States*

**Eranthie Weerapana** − *Department of Chemistry, Boston College, Chestnut Hill, Massachusetts 02467, United States;* orcid.org/0000-0002-0835-8301

**Michael A. Fischbach** − *Department of Bioengineering and ChEM-H, Stanford University, Stanford, California 94305, United States*

Complete contact information is available at: https://pubs.acs.org/10.1021/acsinfecdis.0c00095


### Notes

The authors declare no competing financial interest.

## ■ ACKNOWLEDGMENTS

L.J.K. was supported by the Stanford ChEM-H Chemistry/Biology Interface Predoctoral Training Program, a Stanford Molecular Pharmacology Training Grant, and a Stanford Graduate Fellowship. C.S.L. was supported through a postdoctoral research fellowship by the German Research Foundation (DFG). Y.E.C. was supported by an A.P. Giannini Foundation Postdoctoral Research Fellowship and an HHMI Hanna H. Gray Fellowship. This work was supported by National Institutes of Health grants R01 EB026332 and R01 EB026285 to M.B., R01 DK110174 and R01 DK113598 to M.A.F., and R01GM117004 and R01GM118431 to E.W.

## ■ ABBREVIATIONS

ABPP, activity-based protein profiling; FP, fluorophosphonate; Fph, fluorophosphonate-binding hydrolase; 4-MU, 4-methylumbelliferone; RFU, relative fluorescent unit; CFU, colony-forming unit; TSB, tryptic soy broth; BHI, brain-heart infusion

## ■ REFERENCES


(1) Kloos, W. E., and Musselwhite, M. S. (1975) Distribution and Persistence of *Staphylococcus* and *Micrococcus* Species and Other Aerobic Bacteria on Human Skin. *Appl. Microbiol. 30*, 381−395.

(2) Oh, J., Byrd, A. L., Deming, C., Conlan, S., NISC Comparative Sequencing Program, Kong, H. H., and Segre, J. A. (2014) Biogeography and Individuality Shape Function in the Human Skin Metagenome. *Nature 514*, 59−64.

(3) Grice, E. A., and Segre, J. A. (2011) The Skin Microbiome. *Nat. Rev. Microbiol. 9*, 244−253.

(4) Human Microbiome Project Consortium. (2012) Structure, Function and Diversity of the Healthy Human Microbiome. *Nature 486*, 207−214.

(5) Grice, E. A., Kong, H. H., Conlan, S., Deming, C. B., Davis, J., Young, A. C., NISC Comparative Sequencing Program, Bouffard, G. G., Blakesley, R. W., Murray, P. R., Green, E. D., Turner, M. L., and Segre, J. A. (2009) Topographical and Temporal Diversity of the Human Skin Microbiome. *Science 324*, 1190−1192.

(6) Tong, S. Y. C., Davis, J. S., Eichenberger, E., Holland, T. L., and Fowler, V. G. (2015) *Staphylococcus aureus* Infections: Epidemiology, Pathophysiology, Clinical Manifestations, and Management. *Clin. Microbiol. Rev. 28*, 603−661.

(7) Massey, R. C., Horsburgh, M. J., Lina, G., Höök, M., and Recker, M. (2006) The Evolution and Maintenance of Virulence in *Staphylococcus aureus*: A Role for Host-to-Host Transmission? *Nat. Rev. Microbiol. 4*, 953−958.

(8) Otto, M. (2009) *Staphylococcus epidermidis*–the "Accidental" Pathogen. *Nat. Rev. Microbiol. 7*, 555−567.

(9) Gomes, F., Teixeira, P., and Oliveira, R. (2014) Mini-Review: *Staphylococcus epidermidis* as the Most Frequent Cause of Nosocomial Infections: Old and New Fighting Strategies. *Biofouling 30*, 131−141.

(10) Miragaia, M., Thomas, J. C., Couto, I., Enright, M. C., and de Lencastre, H. (2007) Inferring a Population Structure for *Staphylococcus epidermidis* from Multilocus Sequence Typing Data. *J. Bacteriol. 189*, 2540−2552.

(11) Méric, G., Mageiros, L., Pensar, J., Laabei, M., Yahara, K., Pascoe, B., Kittiwan, N., Tadee, P., Post, V., Lamble, S., Bowden, R., Bray, J. E., Morgenstern, M., Jolley, K. A., Maiden, M. C. J., Feil, E. J., Didelot, X., Miragaia, M., de Lencastre, H., Moriarty, T. F., Rohde, H., Massey, R., Mack, D., Corander, J., and Sheppard, S. K. (2018) Disease-Associated Genotypes of the Commensal Skin Bacterium *Staphylococcus epidermidis*. *Nat. Commun. 9*, 5034.

(12) Conlan, S., Mijares, L. A., NISC Comparative Sequencing Program, Becker, J., Blakesley, R. W., Bouffard, G. G., Brooks, S., Coleman, H., Gupta, J., Gurson, N., Park, M., Schmidt, B., Thomas, P. J., Otto, M., Kong, H. H., Murray, P. R., and Segre, J. A. (2012) *Staphylococcus epidermidis* Pan-Genome Sequence Analysis Reveals Diversity of Skin Commensal and Hospital Infection-Associated Isolates. *Genome Biol. 13*, R64.

(13) Espadinha, D., Sobral, R. G., Mendes, C. I., Méric, G., Sheppard, S. K., Carriço, J. A., de Lencastre, H., and Miragaia, M. (2019) Distinct Phenotypic and Genomic Signatures Underlie Contrasting Pathogenic Potential of *Staphylococcus epidermidis* Clonal Lineages. *Front. Microbiol. 10*, 1971.

(14) Keller, L. J., Babin, B. M., Lakemeyer, M., and Bogyo, M. (2020) Activity-Based Protein Profiling in Bacteria: Applications for Identification of Therapeutic Targets and Characterization of Microbial Communities. *Curr. Opin. Chem. Biol. 54*, 45−53.

(15) Liu, Y., Patricelli, M. P., and Cravatt, B. F. (1999) Activity-Based Protein Profiling: The Serine Hydrolases. *Proc. Natl. Acad. Sci. U. S. A. 96*, 14694−14699.

(16) Kidd, D., Liu, Y., and Cravatt, B. F. (2001) Profiling Serine Hydrolase Activities in Complex Proteomes. *Biochemistry 40*, 4005−4015.

(17) Jessani, N., Niessen, S., Wei, B. Q., Nicolau, M., Humphrey, M., Ji, Y., Han, W., Noh, D.-Y., Yates, J. R., Jeffrey, S. S., and Cravatt, B. F. (2005) A Streamlined Platform for High-Content Functional Proteomics of Primary Human Specimens. *Nat. Methods 2*, 691−697.

(18) Hoegl, A., Nodwell, M. B., Kirsch, V. C., Bach, N. C., Pfanzelt, M., Stahl, M., Schneider, S., and Sieber, S. A. (2018) Mining the Cellular Inventory of Pyridoxal Phosphate-Dependent Enzymes with Functionalized Cofactor Mimics. *Nat. Chem. 10*, 1234−1245.

(19) Ortega, C., Anderson, L. N., Frando, A., Sadler, N. C., Brown, R. W., Smith, R. D., Wright, A. T., and Grundner, C. (2016) Systematic Survey of Serine Hydrolase Activity in *Mycobacterium tuberculosis* Defines Changes Associated with Persistence. *Cell Chem. Biol. 23*, 290−298.

(20) Beatty, K. E., Williams, M., Carlson, B. L., Swarts, B. M., Warren, R. M., Van Helden, P. D., and Bertozzi, C. R. (2013) Sulfatase-Activated Fluorophores for Rapid Discrimination of Mycobacterial Species and Strains. *Proc. Natl. Acad. Sci. U. S. A. 110*, 12911−12916.

(21) Chen, L., Keller, L. J., Cordasco, E., Bogyo, M., and Lentz, C. S. (2019) Fluorescent Triazole Urea Activity-Based Probes for the Single-Cell Phenotypic Characterization of *Staphylococcus aureus*. *Angew. Chem., Int. Ed. 58*, 5643−5647.

(22) Hatzios, S. K., Abel, S., Martell, J., Hubbard, T., Sasabe, J., Munera, D., Clark, L., Bachovchin, D. A., Qadri, F., Ryan, E. T., Davis, B. M., Weerapana, E., and Waldor, M. K. (2016) Chemoproteomic

Profiling of Host and Pathogen Enzymes Active in Cholera. *Nat. Chem. Biol. 12*, 268−274.
(23) Lentz, C. S., Sheldon, J. R., Crawford, L. A., Cooper, R., Garland, M., Amieva, M. R., Weerapana, E., Skaar, E. P., and Bogyo, M. (2018) Identification of a *S. aureus* Virulence Factor by Activity-Based Protein Profiling (ABPP). *Nat. Chem. Biol. 14*, 609−617.
(24) Sugimoto, S., Iwamoto, T., Takada, K., Okuda, K.-I., Tajima, A., Iwase, T., and Mizunoe, Y. (2013) *Staphylococcus epidermidis* Esp Degrades Specific Proteins Associated with *Staphylococcus aureus* Biofilm Formation and Host-Pathogen Interaction. *J. Bacteriol. 195*, 1645−1655.
(25) Cogen, A. L., Yamasaki, K., Sanchez, K. M., Dorschner, R. A., Lai, Y., MacLeod, D. T., Torpey, J. W., Otto, M., Nizet, V., Kim, J. E., and Gallo, R. L. (2010) Selective Antimicrobial Action is Provided by Phenol-Soluble Modulins Derived from *Staphylococcus epidermidis*, a Normal Resident of the Skin. *J. Invest. Dermatol. 130*, 192−200.
(26) Lai, Y., Di Nardo, A., Nakatsuji, T., Leichtle, A., Yang, Y., Cogen, A. L., Wu, Z.-R., Hooper, L. V., Schmidt, R. R., von Aulock, S., Radek, K. A., Huang, C.-M., Ryan, A. F., and Gallo, R. L. (2009) Commensal Bacteria Regulate Toll-like Receptor 3-Dependent Inflammation after Skin Injury. *Nat. Med. 15*, 1377−1382.
(27) Naik, S., Bouladoux, N., Wilhelm, C., Molloy, M. J., Salcedo, R., Kastenmuller, W., Deming, C., Quinones, M., Koo, L., Conlan, S., Spencer, S., Hall, J. A., Dzutsev, A., Kong, H., Campbell, D. J., Trinchieri, G., Segre, J. A., and Belkaid, Y. (2012) Compartmentalized Control of Skin Immunity by Resident Commensals. *Science 337*, 1115−1119.
(28) Chen, Y. E., Bouladoux, N., Hurabielle, C., Mattke, A. M., Belkaid, Y., and Fischbach, M. A. (2019) Decoding Commensal-Host Communication through Genetic Engineering of *Staphylococcus epidermidis bioRxiv*, 664656, DOI: 10.1101/664656.
(29) Bowden, M. G., Visai, L., Longshaw, C. M., Holland, K. T., Speziale, P., and Höök, M. (2002) Is the GehD Lipase from *Staphylococcus epidermidis* a Collagen Binding Adhesin? *J. Biol. Chem. 277*, 43017−43023.
(30) Simons, J.-W. F. A., van Kampen, M. D., Riel, S., Götz, F., Egmond, M. R., and Verheij, H. M. (1998) Cloning, Purification and Characterisation of the Lipase from *Staphylococcus epidermidis*: Comparison of the Substrate Selectivity with Those of Other Microbial Lipases. *Eur. J. Biochem. 253*, 675−683.
(31) Wang, C., Li, M., Dong, D., Wang, J., Ren, J., Otto, M., and Gao, Q. (2007) Role of ClpP in Biofilm Formation and Virulence of *Staphylococcus epidermidis*. *Microbes Infect. 9*, 1376−1383.
(32) Ohara-Nemoto, Y., Ikeda, Y., Kobayashi, M., Sasaki, M., Tajika, S., and Kimura, S. (2002) Characterization and Molecular Cloning of a Glutamyl Endopeptidase from *Staphylococcus epidermidis*. *Microb. Pathog. 33*, 33−41.
(33) Gardner, S. N., Slezak, T., and Hall, B. G. (2015) kSNP3.0: SNP Detection and Phylogenetic Analysis of Genomes without Genome Alignment or Reference Genome. *Bioinformatics 31*, 2877−2878.
(34) Arpigny, J. L., and Jaeger, K. E. (1999) Bacterial Lipolytic Enzymes: Classification and Properties. *Biochem. J. 343*, 177−183.
(35) Lenfant, N., Hotelier, T., Velluet, E., Bourne, Y., Marchot, P., and Chatonnet, A. (2012) ESTHER, the Database of the $\alpha/\beta$-Hydrolase Fold Superfamily of Proteins: Tools to Explore Diversity of Functions. *Nucleic Acids Res. 41*, D423−D429.
(36) Naik, S., Bouladoux, N., Linehan, J. L., Han, S.-J., Harrison, O. J., Wilhelm, C., Conlan, S., Himmelfarb, S., Byrd, A. L., Deming, C., Quinones, M., Brenchley, J. M., Kong, H. H., Tussiwand, R., Murphy, K. M., Merad, M., Segre, J. A., and Belkaid, Y. (2015) Commensal-Dendritic-Cell Interaction Specifies a Unique Protective Skin Immune Signature. *Nature 520*, 104−108.
(37) Linehan, J. L., Harrison, O. J., Han, S.-J., Byrd, A. L., Vujkovic-Cvijin, I., Villarino, A. V., Sen, S. K., Shaik, J., Smelkinson, M., Tamoutounour, S., Collins, N., Bouladoux, N., Dzutsev, A., Rosshart, S. P., Arbuckle, J. H., Wang, C.-R., Kristie, T. M., Rehermann, B., Trinchieri, G., Brenchley, J. M., O'Shea, J. J., and Belkaid, Y. (2018) Non-Classical Immunity Controls Microbiota Impact on Skin Immunity and Tissue Repair. *Cell 172*, 784−796.
(38) Grice, E. A. (2015) The Intersection of Microbiome and Host at the Skin Interface: Genomic- and Metagenomic-Based Insights. *Genome Res. 25*, 1514−1520.
(39) Ansong, C., Ortega, C., Payne, S. H., Haft, D. H., Chauvignè-Hines, L. M., Lewis, M. P., Ollodart, A. R., Purvine, S. O., Shukla, A. K., Fortuin, S., Smith, R. D., Adkins, J. N., Grundner, C., and Wright, A. T. (2013) Identification of Widespread Adenosine Nucleotide Binding in *Mycobacterium tuberculosis*. *Chem. Biol. 20*, 123−133.
(40) Weerapana, E., Speers, A. E., and Cravatt, B. F. (2007) Tandem Orthogonal Proteolysis-Activity-Based Protein Profiling (TOP-ABPP) - A General Method for Mapping Sites of Probe Modification in Proteomes. *Nat. Protoc. 2*, 1414−1425.


https://dx.doi.org/10.1021/acsinfecdis.0c00095
*ACS Infect. Dis.* 2020, 6, 930−938